# Globally Stable Attitude Control of a Fixed-Wing Rudderless UAV Using Subspace Projection

Yujendra Mitikiri and Kamran Mohseni

***Abstract*—This letter extends recent work on globally asymptotically stable nonlinear attitude control of fully actuated vehicles to underactuated vehicles, specifically, a rudderless fixed-wing airplane. Previous work uses a quaternion attitude representation and Lyapunov theory to establish global asymptotic stability for attitude tracking in a fully actuated fixed-wing airplane, beginning from arbitrary initial conditions. Many small unmanned aerial vehicles are, however, heavily constrained with respect to sensor and actuator resources. A common situation is a flying wing configuration with a pair of elevons that serve the purpose of both the elevator as well as the ailerons. While it is not possible to track an arbitrary attitude in the three-dimensional (3-D) attitude space, we show that it is still possible to track a 2-D subspace of the unit quaternion space. Projecting a desired attitude onto a 2-D subspace is achieved by solving an optimization problem in the quaternion attitude formulation. The resulting controller is verified using simulations that demonstrate satisfactory performance.**

***Index Terms*—Aerial systems, mechanics and control, underactuated robots, robust/adaptive control of robotic systems.**

## I. Introduction

THE attitude dynamics of a fixed wing airplane are primarily nonlinear. If the deviations from trimmed conditions are relatively small, the dynamics may be linearized to perform a perturbation analysis about the nominal trimmed motion. The small perturbation assumption is the key to enabling a linear analysis that yields to classical methods of linear feedback control. Implicit in this treatment are the understated and frequently overlooked secondary assumptions that the initial conditions are also close to the trim conditions, and that external disturbances do not cause the system to move far away from such conditions. These may hold true for large aircraft flying at high speeds, which have a high inertia and present a relatively small exposure to environmental disturbances at the boundary (note: if $L$ is a characterstic length associated with a vehicle, inertia scales as $L^3$, while the surface area exposed to the environment scales as $L^2$). For smaller vehicles flying at low speeds, the effect of environmental disturbances can no longer be ignored. For instance, external wind may cause increasingly larger perturbations in the angle-of-attack, $\alpha$, and sideslip angle, $\beta$. These perturbations would in turn cause the attitude state to move far away from the trim conditions, such that the linearized analysis is no longer valid and the controller fails to track or stabilize the vehicle.

A second non ideality occurs on account of the coupling between the lateral and longitudinal dynamics of low aspect ratio wings. It has been experimentally observed that wing-tip vortices can cause the sideslip-roll stability derivative ($C_{l,\beta}$) to be a strong function of $\alpha$, in effect causing the roll moment to vary both with respect to $\alpha$ as well as $\beta$ [1]. In other words, the lateral state variable roll rate $p$ has a stability derivative with respect to the longitudinal variable $\alpha$.

The above nonidealities motivate a new approach to the control of small unmanned aerial vehicles (UAVs), that places greater emphasis on the control of the coupled attitude dynamics of the vehicle, while also accounting for external disturbances. There is very little published work on attitude control in fixed wing aircraft that ensures global asymptotic stability (GAS), while also estimating, and accounting for, the effect of external wind on the attitude dynamics. Most work focus exclusively on the attitude control problem [2]–[5], or the aerodynamic angle estimation problem [6]–[8]. In [9], the authors present a novel attitude controller that accounts for both the nonidealities, by designing a single integrated nonlinear attitude controller that accounts for the coupled lateral-longitudinal dynamics, and is GAS with respect to initial conditions and deviations from trimmed motion.

One of the assumptions in the controller presented in [9] is that the airplane is fully actuated. For fixed-wing airplanes, this translates to the requirement of three independent degrees of control, traditionally the roll, pitch, and yaw controllers actuating the ailerons, elevator, and rudder respectively. When all three actuations are present and effective, the airplane can be controlled to track any arbitrary attitude configuration (asymptotic stability), beginning from any arbitrary initial condition (global nature of the stability). Note that the three actuation degrees are independent and effective only when the airplane is not under stall, actuator saturation, or similar pathological conditions.

In the absence of a fully-actuated vehicle, it is, in general, not possible to track any arbitrary attitude configuration in the full three-dimensional attitude space. For instance, the specification

Manuscript received September 10, 2018; accepted January 9, 2019. Date of publication January 29, 2019; date of current version February 15, 2019. This letter was recommended for publication by Associate Editor V. Lippiello and Editor J. Roberts upon evaluation of the reviewers' comments. This work was supported in part by NSF, in part by the Air Force Office of Scientific Research and in part by the Office of Naval Research. *(Corresponding author: Kamran Mohseni.)*

Y. Mitikiri is with the Department of Mechanical and Aerospace Engineering, University of Florida, Gainesville, FL 32611 USA (e-mail: yujendra@ufl.edu).

K. Mohseni is with the Department of Mechanical and Aerospace Engineering, and Department of Electrical and Computer Engineering, University of Florida, Gainesville, FL 32611 USA (e-mail: mohseni@ufl.edu).

This paper has supplementary downloadable material available at http://ieeexplore.ieee.org, provided by the authors.

Digital Object Identifier 10.1109/LRA.2019.2895889

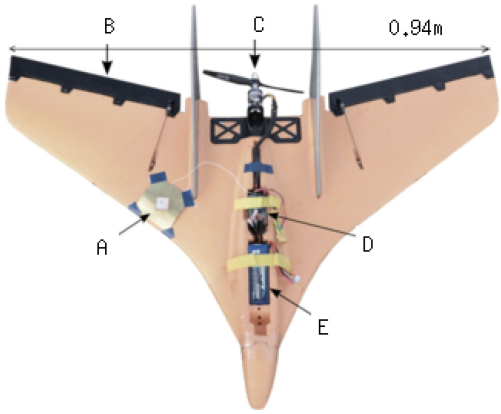


Fig. 1. The Stryker F27 rudderless deltawing with a pair of elevons. The wing span is 0.94 m and the fully loaded weight is 0.66 kg. A. GPS antenna, B. Elevon, C. Propeller, D. Autopilot from [10], E. Battery.

of a constant positive roll angle in a typical fixed-wing rudderless airplane leads to a constant positive yaw-rate, and the yaw angle can no longer be independently specified. Conversely, the specification of a yaw-rate yields a specification on the roll attitude in such an airplane. This situation (of being under-actuated) is quite common in the field of small unmanned aerial vehicles (UAVs), which are highly constrained with respect to available sensor and actuator resources. Such is the case with, for example, the 0.94 m-span Stryker F27 fixed deltawing (Fig. 1) small RC plane. While this particular model is very convenient on account of its small size, low cost, and robust physical frame, it is associated with the shortcoming of lacking a rudder actuation. Thus we are motivated to extend the GAS attitude controller for the fully actuated case, to the under-actuated case, in particular, a rudderless fixed-wing airplane.

There has been some work reported on the control of under-actuated UAVs in the past. In [11], and [12], aeroelastic and piezoelectric surfaces are used to control rudderless airplanes. In [13], PID controllers are used to control a rudderless airplane. However, as is usual with linear control methods, the airplane is assumed to never perform major excursions from the trim conditions.

There are several nonlinear controllers that achieve near GAS for under-actuated UAVs, but most of them involve rotorcraft [14], [15], [16], [17], and the methods reported do not easily extend to fixed-wing airplanes. For example, the under-actuation in rotorcrafts involves the composite translational and rotational dynamics, while the under-actuation in fixed-wing airplanes is almost always specific to the rotational dynamics (exceptions include gliders without propulsion). Furthermore, the physical quantities of significance in the dynamics of fixed-wing airplanes differ from those in rotorcraft. The work in [14] does not consider disturbances in the aerodynamic angles, as these are not a major concern in the control of rotorcraft UAVs. However, the aerodynamic angles, angle of attack $\alpha$ and sideslip $\beta$, play a major role in the dynamics of fixed-wing aircraft and disturbances introduced through them cannot be ignored for such aircraft. Similarly, The work in [17] considers bounded uncertainties, but does not consider aerodynamic damping proportional to the angular velocity. Thus, the absence of a suitable controller for fixed-wing under-actuated airplanes in existing literature motivates the extension of the GAS nonlinear controller in [9].

A brief outline of this letter is as follows: the next section discusses the background of the problem, including the vehicle dynamics, and GAS attitude control. Section III contains the main technical contribution in this letter: the derivation of a consistent subspace of reference attitudes for an underactuated airplane, within which the stability results apply. Section IV presents simulation results validating the presented solution, leading to the final conclusion.

## II. Globally Stable Nonlinear Attitude Control

We consider a fixed-wing airplane with attitude dynamics given by (*e.g.*, [9]):

$$\dot{\breve{q}} = \frac{1}{2}\breve{q} \otimes \omega = \frac{1}{2}\begin{bmatrix} -q_1 & -q_2 & -q_3 \\ q_0 & -q_3 & q_2 \\ q_3 & q_0 & -q_1 \\ -q_2 & q_1 & q_0 \end{bmatrix}\begin{bmatrix} p \\ q \\ r \end{bmatrix} = \frac{1}{2}A^T\omega, \quad (1)$$

where $\breve{q} = [q_0\ q_1\ q_2\ q_3]^T$ denotes the 4-component attitude quaternion of unit magnitude, $\omega = [p\ q\ r]^T$ denotes the angular velocity of the airplane in the body frame and $\otimes$ signifies quaternion multiplication. The aileron, elevator and rudder control inputs enters the dynamics through the equations of motion for angular accelerations:

$$\dot{\omega} = D + G(H + I\omega + J\delta)\ , \quad (2)$$

where, $D = M^{-1}\omega \times M\omega$ contains the contribution due to the rotating body frame; $G$ is a scaled inverse of the moments of inertia matrix $M$; $J$ is the matrix of control derivatives; $\delta = [\delta_a,\ \delta_e,\ \delta_r]^T$ is the control input from the ailerons, elevator, and rudder; $H$ is the coupling from the translational variables $\alpha$ and $\beta$ into attitude dynamics; $I$ is the matrix of damping derivatives. Given these nonlinear dynamics, the control inputs in a GAS controller are derived in [9]:

$$GJ\delta = -(D + GH + GI\omega) + 2A(L_1^2 e_1 - (L_1 + L_2)e_2 + \dddot{\breve{q}}_r) - 2\dot{A}e_2\ , \quad (3)$$

where, $e_1 = \breve{q} - \breve{q}_r$ and $e_2 = \dot{e}_1 + L_1 e_1$ are the tracking and filtered tracking error with respect to the reference attitude $\breve{q}_r$, and $L_1$ and $L_2$ are positive definite gain matrices.

It can be seen from (3) that the control is well defined only when the control-derivative matrix $J$ is of rank 3 and invertible, *i.e.*, the airplane is fully actuated. A typical $J$ would contain derivatives of the roll, pitch, and yaw moments with respect to the control inputs, for example:

$$J = \begin{bmatrix} C_{l,\delta a} & 0 & C_{l,\delta r} \\ 0 & C_{m,\delta e} & 0 \\ C_{n,\delta a} & 0 & C_{n,\delta r} \end{bmatrix}, \quad (4)$$

with lateral and longitudinal control separation. In a rudderless airplane with two degrees of actuation, the matrix $J$ in equation (3) would contain only the first and second columns. In this situation, $J$ has a nonzero nullspace spanned by a vector $f$. In

the above example with lateral-longitudinal control separation, $f$ would lie along $[-C_{n,\delta a}\ 0\ C_{l,\delta a}]^T$ so that

$$f^T J = \begin{bmatrix} -C_{n,\delta a} & 0 & C_{l,\delta a} \end{bmatrix} \begin{bmatrix} C_{l,\delta a} & 0 \\ 0 & C_{m,\delta e} \\ C_{n,\delta a} & 0 \end{bmatrix} = 0\ . \quad (5)$$

The vector $f$ would in general depend upon the coefficients in matrix $J$, and we shall assume that $f$ is known in our controller design. Thus, the right hand side in equation (3) is constrained on account of under-actuation to satisfy

$$f^T R = 0, \quad (6)$$

where $GR = -(D + GH + GI\omega) + 2A(L_1^2 e_1 - (L_1 + L_2)\ e_2 + \ddot{\breve{q}}_r)$ is the right hand side of equation (3). Equation (6) provides one scalar degree of constraint on the evolution of the reference attitude $\breve{q}_r$ with time.

One approach to design the underactuated controller is to employ least-squares to solve for the control $\delta$:

$$\delta = (J^T J)^{-1} J^T G^{-1} R\ , \quad (7)$$

where, $R$ is the RHS of equation (3). The Lyapunov analysis that provided the stability results in the fully actuated case is no longer applicable, but for small deviations from a prescribed trajectory, a linearized analysis shows that equation (7) still provides stable attitude tracking. However, this approach no longer provides the GAS result of the fully actuated situation. Since this is not the approach taken in this letter, we do not discuss it further.

Another approach for globally stable attitude control in underactuated vehicles is to derive the reference attitude $\breve{q}_r$ in such a manner that the RHS in equation (3) degenerates into a two-dimensional subspace, so that it can be uniquely solved even in the underactuated case. This precludes the access of all points in the general three-dimensional attitude space. With this caveat, we are once again guaranteed GAS attitude control by taking this approach. It may be noted that the restriction to a two-dimensional attitude subspace still allows the accessibility of a three-dimensional velocity space to the airplane. This access is provided by the attitude and throttle control. With this clarification, we proceed to derive such a reference attitude trajectory in the next section.

## III. Attitude Projection and Yaw Correction

As discussed in the previous section, it is not possible to orient a fixed-wing airplane in an arbitrary attitude configuration by actuating only the ailerons and elevator. Intuitively, we can see that two independent controls cannot access all three degrees of freedom of an arbitrary attitude. We next note that the ailerons produce a primarily rolling moment, while the elevator produces a primarily pitching moment. Furthermore, the yaw angle is a cyclic variable in the flight dynamics of a fixed-wing airplane. We are therefore led to considering the problem of projecting a desired attitude onto a two-dimensional subspace specified only by the roll and pitch angles.

Let us denote the three dimensional space of all rigid body attitude configurations by $\mathbb{Q}$. We shall refer to the subspace with a roll-pitch specification as the free-yaw subspace $\mathbb{Q}_\psi$. Attitudes in $\mathbb{Q}$ shall be denoted by variables with a check accent, for *e.g.*, $\breve{p}, \breve{q}$ *etc*.

The naive method of projecting from a given attitude $\breve{p}$ onto the free-yaw subspace of a second attitude $\breve{q}$ might seem to be to retain the yaw angle from $\breve{p}$, and changing the roll and pitch angles to those given by $\breve{q}$. However, as we demonstrate below using a counter example, this is not the most efficient strategy in projecting from one attitude onto another subspace.

Consider, for example, an airplane in the 321 Euler angle attitude $\breve{p} = [0, \pi/2 - \delta, \pi/2]$ that needs to be projected onto the free-yaw subspace $\mathbb{Q}_\psi = [\psi, \pi/2 - \delta, -\pi/2]$, where $0 < \delta \ll \pi/2$, and $\psi$ is unspecified and free. Retaining the yaw angle from $\breve{p}$, and the roll and pitch angles from $\breve{q}$ yields the attitude $[0, \pi/2 - \delta, -\pi/2]$, thus requiring a rotation through $\pi$ about the body roll axis. Instead consider the projection onto $\breve{r} = [\pi, \pi/2 - \delta, -\pi/2]$. While the sequential rotations from the $[0, 0, 0]$ configuration to $\breve{p}$ and $\breve{r}$ differ by $\pi$ along the yaw axis, and subsequently by $\pi$ along the roll axis, the incremental rotation in going from $\breve{p}$ to $\breve{r}$ is only $2\delta$ along the body yaw axis, and is much smaller than the rotation through $\pi$ in going from $\breve{p}$ to $\breve{q}$. Therefore, if done correctly, projecting from $\breve{p}$ to $\breve{r}$ is much more efficient than projecting from $\breve{p}$ to $\breve{q}$.

The above example shows that the Euler angle representation might not be the best way to compare two rotations. A much better representation is one using unit quaternions. The quaternion representations of $\breve{p}, \breve{q}, \breve{r}$ in the above example are $[(1+\delta),\ (1+\delta),\ (1-\delta),\ -(1-\delta)]^T/2$, $[(1+\delta),\ -(1+\delta),\ (1-\delta),\ (1-\delta)]^T/2$, and $[-(1-\delta),\ -(1-\delta),\ -(1+\delta),\ (1+\delta)]^T/2$ respectively. The rotation that takes $\breve{p}$ to $\breve{q}$ is given by $\breve{p}^{-1} \otimes \breve{q} = [0,\ -1,\ 0,\ 0]^T$, while the rotation that takes $\breve{p}$ to $\breve{r}$ is given by $\breve{p}^{-1} \otimes \breve{r} = [1,\ 0,\ 0,\ 2\delta]^T$, where $\otimes$ denotes quaternion multiplication, and we have made the approximation that $\delta \ll 1$. In this representation, it is clear that the most efficient projection of $\breve{p}$ on the free-yaw subspace $\mathbb{Q}_\psi$ is given by $\breve{r}$.

Consider now the attitude of an airplane $\breve{q}$ in the quaternion representation that needs to track a reference attitude quaternion $\breve{q}_r$. We would like to specify the reference attitude $\breve{q}_r$ such that its dynamics are consistent with the rank-deficiency of matrix $J$, but at the same time, it leads to a desired roll and pitch specification $\phi_r$ and $\theta_r$. The projection of an attitude $\breve{p}_r$ onto a free yaw subspace has been reported in [18] and is given by:

$$\breve{q}_r = \begin{bmatrix} p_{r0} \\ p_{r1} \\ p_{r2} \\ p_{r3} \end{bmatrix} = \frac{1}{\sqrt{2(1+\kappa^2)(1+b_3)}} \begin{bmatrix} \kappa(1+b_3) \\ \kappa b_2 + b_1 \\ -\kappa b_1 + b_2 \\ (1+b_3) \end{bmatrix}, \quad (8)$$

where,

$$\begin{bmatrix} b_1 \\ b_2 \\ b_3 \end{bmatrix} = \begin{bmatrix} -\sin\theta_r \\ \cos\theta_r \sin\phi_r \\ \cos\theta_r \cos\phi_r \end{bmatrix},$$

$$\kappa = \frac{(1+b_3)p_0 - b_1 p_2 + b_2 p_1}{b_1 p_1 + b_2 p_2 + (1+b_3)p_3}\ . \quad (9)$$

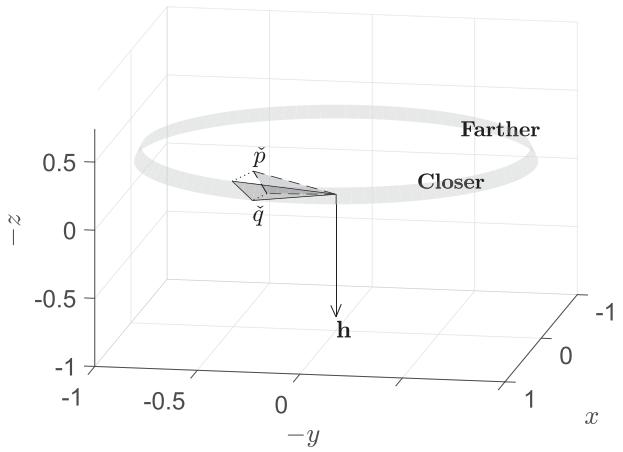


Fig. 2. Projection of the attitude of a minimal rigid body (represented by the triangular patch) onto the free-yaw subspace using equations (8) and (9) [18].

The projection is visually depicted in Figure 2.

The optimal static projection of the reference attitude described above, from $\check{p}_r(t)$ at time $t$ to $\check{q}_r(t+dt)$ at $t+dt$, is appropriate for negligible angular velocities, *i.e.*, when $\omega_r \approx 0$, and the yaw angle is free (hence the terminology). When a nonzero reference angular velocity or acceleration is desired, the attitude dynamics are to additionally satisfy equations (1) and (2). Moreover, in an under-actuated airplane, the projected attitude $\check{q}_r$ may give rise to an attitude trajectory that is inconsistent with respect to the constraint equation (6). These requirements are satisfied by following a three-step sequential algorithm in time, that we describe next.

The first step is to determine a nominal reference attitude $\check{p}_r$, reference angular velocity $\nu_r$, and reference angular acceleration $\alpha_r$, that can be reached with no control effort. The angular acceleration $\alpha_r$ is nominally determined from equation (2) for zero errors $e_1$ and $e_2$, and zero control effort $\delta$:

$$\alpha_r = \dot{\omega}_r = D_r + GH + GI\omega_r, \tag{10}$$

where $D_r = M^{-1}(\omega_r \times M\omega_r)$ is the kinematic transport term for the reference trajectory. We set the errors to zero as we are deriving the reference trajectory. The control effort is set to zero in order to derive the natural dynamics of the airplane in the reference attitude, and also to remain unbiased at this stage. Integration of equations (10) and (1) then yield a nominal evolution for the reference angular velocity and attitude quaternion in time:

$$\begin{bmatrix} \nu_r(t+dt) \\ \check{p}_r(t+dt) \end{bmatrix} = \begin{bmatrix} \omega_r(t) + \alpha_r(t+dt)dt \\ \check{q}_r(t) + \frac{dt}{2}\check{q}_r(t) \otimes \nu_r(t+dt) \end{bmatrix}. \tag{11}$$

It must be noted that the integrated angular velocity $\nu_r$ and attitude $\check{p}_r$ are only nominal, and subject to change as described below. We shall therefore denote the actual reference attitude, angular velocity and acceleration at time $t+dt$ by using different symbols $\check{q}_r$, $\omega_r$, and $\beta_r$. The nominal reference acceleration $\alpha_r$ in equation (10) is the optimal value if there was no tracking objective, or control constraint. The presence of a tracking objective (of tracking a desired roll and pitch specification) and a control constraint (of being under-actuated), entail a modification to $\alpha_r(t+dt)$. A similar comment applies to $\nu_r(t+dt)$ and $\check{p}_r(t+dt)$.

The second step in deriving the reference trajectory is to incorporate the desired roll and pitch angles $\phi_r(t+dt)$ and $\theta_r(t+dt)$. To this end, we project the integrated attitude $\check{p}_r(t+dt)$ onto $\check{r}_r(t+dt)$ in the free yaw subspace specified by $\phi_r$ and $\theta_r$ using equations (8) and (9). The projection from $\check{p}_r$ to $\check{r}_r$ is optimal with respect to meeting the roll and pitch angle specifications when there is no other constraint equation. If there was no control constraint this would be our reference attitude at time $t+dt$.

A third and final step in determining the reference attitude at time $t+dt$ is in order to comply with the under-actuation constraint contained in equation (6), so that we can solve for a suitable control command using equation (3) that provides GAS attitude tracking. We shall therefore correct $\check{r}_r(t+dt)$ by a suitable yaw angle $\psi_c$ to the final attitude configuration $\check{q}_r(t+dt)$ in order to meet the under-actuation constraint:

$$\check{q}_r(t+dt) = \check{h}_c \otimes \check{r}_r(t+dt), \tag{12}$$

where $\check{h}_c = [\cos(\psi_c/2)\ 0\ 0\ \sin(\psi_c/2)]^T$ is the yaw-correction to $\check{r}_r$ and $\psi_c$ is undetermined as yet.

The constraint-corrected reference attitude $\check{q}_r$ can be reached only by changing the nominal angular velocity $\nu_r$ in equation (11) to the final angular velocity $\omega_r$, which in turn requires a change in the nominal acceleration $\alpha_r$ to $\beta_r$:

$$\begin{bmatrix} \omega_r(t+dt) \\ \beta_r(t+dt) \end{bmatrix} = \begin{bmatrix} 2\check{q}_r^{-1}(t) \otimes (\check{q}_r(t+dt) - \check{q}_r(t))/dt \\ (\omega_r(t+dt) - \omega_r(t))/dt \end{bmatrix} \tag{13}$$

In order to derive the appropriate yaw-correction $\psi_c$, we substitute $\check{q}_r(t+dt)$ and $\omega_r(t+dt)$ in equation (6). It may be recalled that the error variables $e_1$ and $e_2$ contain $\check{q}_r$ and $\dot{\check{q}}_r$, and also the airplane's attitude $\check{q}$ and $\dot{\check{q}}$. The resulting scalar equation may then be solved for the single unknown $\psi_c$, which completes the specification of the reference attitude $\check{q}_r$ at time $t+dt$, along with the reference angular velocity $\omega_r$, and the reference angular acceleration $\beta_r(t+dt)$.

The entire procedure may be summarized in the following sequential algorithm:

1) Initialize the reference attitude $\check{q}_r(0)$, angular velocity $\omega_r(0)$, and angular acceleration $\beta_r(0)$.
2) Determine the nominal angular acceleration $\alpha_r(t+dt)$ at time $t+dt$ using equation (10). This nominal acceleration would require zero control effort.
3) Determine the nominal angular velocity $\nu_r(t+dt)$ and the nominal attitude $\check{p}_r(t+dt)$ by integrating the nominal angular acceleration $\alpha_r(t+dt)$ and angular velocity $\nu_r(t+dt)$, as given by equation (11).
4) Project the nominal attitude $\check{p}_r(t+dt)$ onto the free-yaw subspace specified by the desired roll and pitch angles $\phi_r(t+dt)$ and $\theta_r(t+dt)$ using equations (8) and (9).
5) Rotate the projected attitude through an undetermined yaw angle $\psi_c$ into $\check{q}_r(t+dt)$ using equation (12) and derive the corresponding angular velocity and acceleration, $\omega_r$ and $\beta_r$, using equation (13).

6) Substitute the values of $\breve{q}_r(t+dt)$, $\dot{\breve{q}}_r(t+dt)$, and $\omega_r(t+dt)$ into the under-actuation constraint equation (6) to solve for the yaw correction $\psi_c$, and hence determine $\breve{q}_r(t+dt)$, $\omega_r(t+dt)$, and $\beta_r(t+dt)$.
7) Repeat steps 2 to 6 until the final time $t_f$.

It must be noted that the GAS controller in equation (3) requires the reference attitude $\breve{q}_r$, and its first and second time derivatives, $\dot{\breve{q}}_r$ and $\ddot{\breve{q}}_r$, to be bounded. These conditions are now transferred to the reference roll and pitch angle specifications: $\dot{\phi}_r$, $\ddot{\phi}_r$, $\dot{\theta}_r$, and $\ddot{\theta}_r$ must be bounded and $|\theta| < \theta_m < \pi/2$ for some constant $\theta_m$ sufficiently far away from $\pi/2$ (note: these conditions apply to the reference attitude and are not to be confused as conditions on the airplane's attitude, which is still arbitrary; the global stability of the controller still provides asymptotic tracking to the bounded reference trajectory for any given initial attitude).

As an example application of the proposed method, the free-yaw subspace for the attitude projection, $\mathbb{Q}_{\psi,i+1}$, may be derived in order to perform waypoint and path tracking missions. For example, the reference roll angle, $\phi_r$, and pitch angle, $\theta_r$, may be determined by the below equations in order to track waypoints:

$$\begin{aligned}\phi_r &= \phi_m \tanh(\psi_r + \psi_0 - \psi) \\ &= \phi_m \tanh(\operatorname{atan}((y-y_r)/(x-x_r)) + \psi_0 \\ &\quad - \operatorname{atan}(2(p_0p_3 + p_1p_2)/(p_0^2 + p_1^2 - p_2^2 - p_3^2))), \quad (14)\end{aligned}$$

$$\theta_r = \theta_m \tanh(z - z_r)/L_z\,, \quad (15)$$

where, $(x, y, z)$ are the current spatial coordinates of the airplane, $(x_r, y_r, z_r)$ are the coordinates of the waypoint, $L_z$ is a length that determines the gain from an error in $z$ to $\theta_r$, and $\phi_m$, and $\theta_m$ are the maximum roll and pitch angles. The translational dynamics of $x$, $y$, and $z$, and the yaw angle $\psi$ are bounded, and consequently so are those of $\phi_r$ and $\theta_r$.

## IV. Simulation Results

In this section, we verify that it is possible to achieve waypoint tracking in a rudderless airplane using the optimal attitude subspace projection and yaw correction described in the previous section. For the simulations, we use the aerodynamic model derived for the Stryker F27C small unmanned aerial vehicle provided in [19]. The Stryker F27C has a wingspan of 0.94 m and a loaded mass of 0.67 kg. The hardware and autopilot are described in [10]. Important geometric, inertial, and aerodynamic properties of the vehicle are provided in [19] and reproduced below in Table I and II.

In the below simulation, the airplane is initialized in an arbitrary attitude at time $t = 0$ and directed to a waypoint at $x_r = 300$, $y_r = -50$ until time $t < 90s$, and subsequently redirected to a new waypoint at $x_r = 200$, $y_r = 150$. Both way points are located at an altitude of $-z_r = 200$. Equations (14) and (15) are used to derive a reference roll and pitch angle at each time instance. The algorithm presented in Section III is then used to derive a reference attitude trajectory for the GAS controller of equation (3).

TABLE I
Geometry and Inertial Parameters of the Stryker F27C Small UAV [19]

| Parameter | Measured value |
|---|---|
| Wing-span $b$ | 0.940 m |
| Reference chord $c$ | 0.270 m |
| Wing planform area $S$ | 0.217 m$^2$ |
| Mass $M$ | 0.66 kg |
| Position of CG $x_{CG}$ | 0.15 m |
| Moment of inertia $I_{xx}$ | 0.0079 kgm$^2$ |
| Moment of inertia $I_{yy}$ | 0.0203 kgm$^2$ |
| Moment of inertia $I_{zz}$ | 0.0282 kgm$^2$ |
| Moment of inertia $I_{xz}$ | 0.0000 kgm$^2$ |
| Air density $\rho$ | 1.2 kg/m$^3$ |
| Airspeed $V_a$ | 12.5 m/s |

TABLE II
Aerodynamic Stability and Control Derivatives of the Stryker F27C UAV, Under Trim Conditions [19]

| Parameter | AVL | Windtunnel |
|---|---|---|
| $C_{m0}$ | -0.018 | |
| $C_{m,\alpha}$ | -0.108 | |
| $C_{m,q}$ | -1.203 | -1.321 |
| $C_{m,\delta_e}$ | -0.264 | |
| $C_{l0}$ | 0.000 | |
| $C_{l,\beta}$ | -0.056 | |
| $C_{l,p}$ | -0.323 | -0.392 |
| $C_{l,r}$ | 0.042 | 0.051 |
| $C_{l,\delta_a}$ | -0.139 | |
| $C_{n0}$ | 0.000 | |
| $C_{n,\beta}$ | 0.049 | |
| $C_{n,p}$ | -0.072 | -0.027 |
| $C_{n,r}$ | -0.025 | -0.027 |
| $C_{n,\delta_a}$ | -0.011 | |

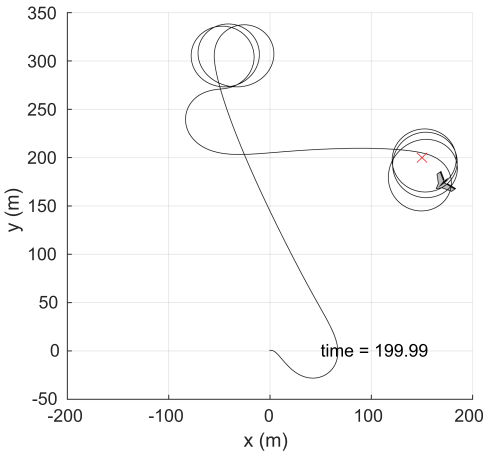


Fig. 3. Ground track of the airplane commanded on a waypoint tracking mission. The waypoint is $(300, -50)$ for time $t < 90s$, and $(200, 150)$ subsequently.

The ground track in Figure 3 shows successful waypoint tracking. The airplane initially heads directly towards the waypoint from a distance. Once it gets close, the sigmoid function in (14) causes it to loiter around the waypoint at the maximum roll angle $\phi_m$. In this simulation $\phi_m$ was set to $\pi/6$, and $\theta_m$ was set to $\pi/18$.

In order to verify global stability, the vehicle is initialized in a random attitude at time $t = 0$. It is seen in Figure 3 that the

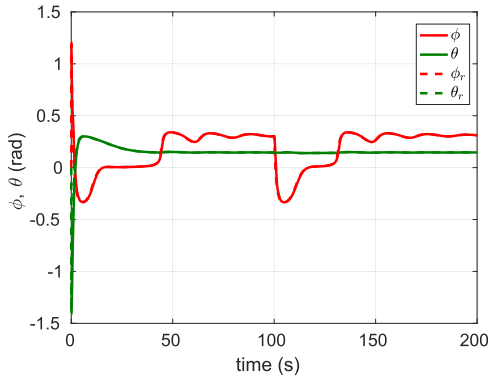


Fig. 4. The airplane commanded on a waypoint tracking mission. Shown in this figure is the asymptotic Euler angle attitude tracking from a random initialization.

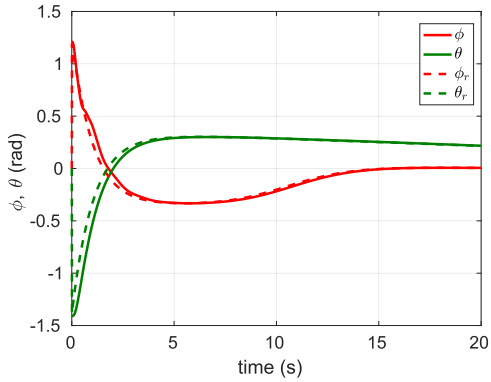


Fig. 5. A zoomed in portion of the attitude tracking at initial time shows large initial errors and the global nature of the stability provided by the controller.

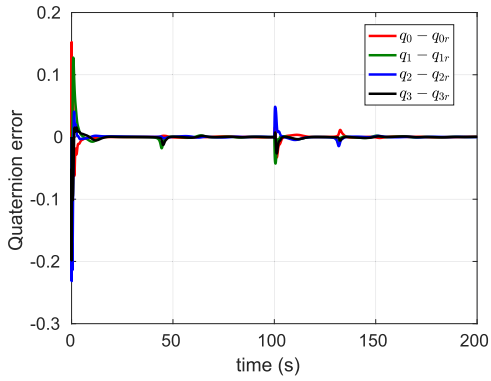


Fig. 6. Quaternion attitude error while tracking waypoints.

airplane is stabilized beginning from initial errors that are as large as $\pi/2$ radians. The large roll angle error causes the initial path of the airplane to not head directly towards the waypoint, as seen in Figure 3. However, within a few seconds, the nonlinear controller stabilizes the roll angle (Figure 4). During the turn, the reference roll angle is suitably modified by equation (14) in order to loiter around the commanded waypoint. As the airplane loses altitude upon banking to turn, the reference pitch angle is modified using equation (15).

Figure 6 shows the asymptotic tracking and Figure 7 shows the bounded control input that provides the tracking performance.

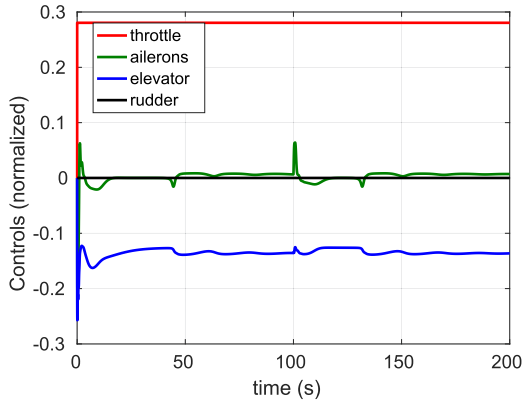


Fig. 7. The normalized control input while tracking waypoints. Note that the rudder input is forced to 0, as the Stryker F27 doesn't have a rudder.

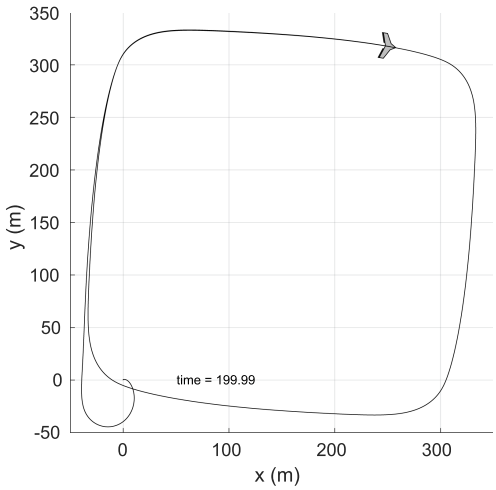


Fig. 8. Ground track of the airplane commanded on a path tracking mission. The target path is a square with corners at $(0, 0)$, $(0, 300)$, $(300, 300)$, and $(300, 0)$.

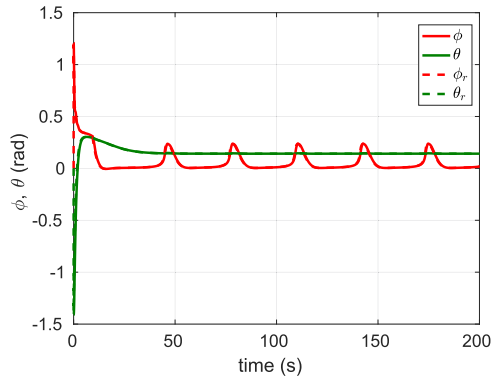


Fig. 9. The airplane commanded on a path tracking mission. Shown in this figure is the asymptotic Euler angle attitude tracking from a random initialization.

The airplane can also be commanded for path tracking missions as shown in the next set of figures (Figs. 8–12). The target path is a square path with corners at $(0, 0)$, $(0, 300)$, $(300, 300)$, and $(300, 300)$, traversed in clockwise sense. As the airplane passes each vertex of the square, its inertia causes it to overshoot the desired trajectory. The controller subsequently causes

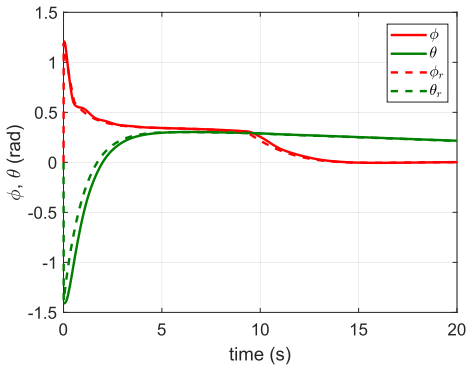


Fig. 10. A zoomed in portion of the attitude tracking at initial time shows large initial errors and the global nature of the stability provided by the controller.

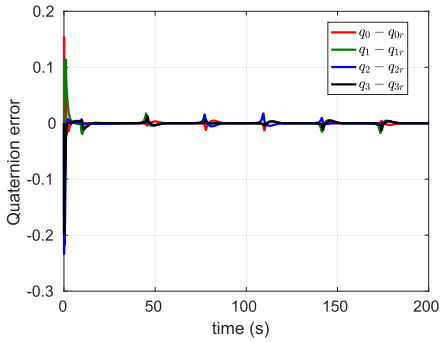


Fig. 11. Quaternion attitude error while tracking the reference path.

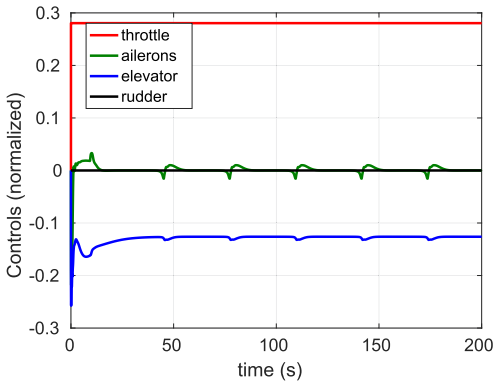


Fig. 12. The normalized control input while tracking the reference path. Note that the rudder input is forced to 0, as the Stryker F27 doesn't have a rudder.

the airplane to bank and turn so as to approach the next target vertex. Once the heading is correct, the controller returns to level flight until the next vertex.

It is straightforward to extend the above procedure from a square path to an arbitrary path, whose curvature is not so steep as to exceed the maximum desired bank angle $\phi_m$, by approximating it as a series of piecewise straight line segments. The minimum radius of curvature can be computed as $R \approx V_a^2/(g \tan \phi_m)$, where $V_a$ is the airspeed of the airplane and $\phi_m$ is the maximum reference roll angle. For example, values of $V_a = 12.5$ m/s and $\phi_m = \pi/6$ produce a minimum radius of curvature of $\approx$26 m. For steady turns about a waypoint, the error in heading is $\pi/2$, which yields (equation (14)) the radius of the turn as $V_a^2/(g \tan(\phi_m \tanh(\pi/2))) \approx 31$ m.

## V. Conclusion

We have thus presented a method to achieve waypoint or path tracking by a rudderless fixed-wing small UAV, by using a nonlinear attitude controller to optimally track a desired attitude specified solely by roll and pitch angles. The third degree of freedom of the attitude is derived so as to satisfy the control constraint which expresses the absence of the rudder. The performance of the controller with such a reference attitude trajectory is verified in Matlab simulations for global stability. Our team is now working on the experimental validation of the global stability results using the UAV platform described in the introduction.

## References

[1] M. Shields and K. Mohseni, "Inherent stability modes of low aspect ratio wings.," *J. Aircr.*, vol. 52, no. 1, pp. 141–155, 2015.
[2] R. E. Mortensen, "A globally stable linear attitude regulator," *Int. J. Control*, vol. 8, no. 3, pp. 297–302, 1968.
[3] J. T-Y. Wen and K. Kreutz-Delgado, "The attitude control problem," *IEEE Trans. Autom. Control*, vol. 36, no. 10, pp. 1148–1162, Oct. 1991.
[4] J. Thienel and R. M. Sanner, "A coupled nonlinear spacecraft attitude controller and observer with an unknown constant gyro bias and gyro noise," *IEEE Trans. Autom. Control*, vol. 48, no. 11, pp. 2011–2015, Nov. 2003.
[5] N. Chaturvedi, A. K. Sanyal, and N. H. McClamroch, "Rigid-body attitude control," *IEEE Control Syst. Mag.*, vol. 31, no. 3, pp. 30–51, Jun. 2011.
[6] S. Popowski and W. Dabrowski, "Measurement and estimation of the angle of attack and the angle of sideslip," *Aviation*, vol. 19, no. 1, pp. 19–24, 2015.
[7] M. Oosterom and R. Babuska, "Virtual sensor for the angle-of-attack signal in small commercial aircraft," in *Proc. IEEE Int. Conf. Fuzzy Syst.*, 2006, pp. 1396–1403.
[8] C. Ramprasadh and H. Arya, "Multistage-fusion algorithm for estimation of aerodynamic angles in mini aerial vehicle," *J. Aircr.*, vol. 49, no. 1, pp. 93–100, 2012.
[9] Y. Mitikiri and K. Mohseni, "Attitude control of micro/mini aerial vehicles and estimation of aerodynamic angles formulated as parametric uncertainties," *IEEE Robot. Autom. Lett.*, vol. 3, no. 3, pp. 2063–2070, Jul. 2018.
[10] A. Bingler and K. Mohseni, "Dual radio autopilot system for lightweight, swarming micro/miniature aerial vehicles," *J. Aeros. Inf. Syst.*, vol. 14, no. 5, pp. 293–306, 2017.
[11] M. Trapani and S. Guo, "Design and analysis of a rudderless aeroelastic fin," *Proc. Institution Mech. Eng., Part G, J. Aerosp. Eng.*, vol. 223, no. 6, pp. 701–710, 2009.
[12] L. L. Gamble and D. J. Inman, "Bioinspired pitch control using a piezoelectric horizontal tail for rudderless UAVs," *Bioinspiration, Biomimetics, Bioreplication VIII*, vol. 10593, 2018, Art. no. 1059303.
[13] M. Liu, G. K. Egan, and F. Santoso, "Modeling, autopilot design, and field tuning of a UAV with minimum control surfaces," *IEEE Trans. Control Syst. Technol.*, vol. 23, no. 6, pp. 2353–2360, Nov. 2015.
[14] D. Lee, T. C. Burg, B. Xian, and D. M. Dawson, "Output feedback tracking control of an underactuated quad-rotor UAV," in *Proc. Amer. Control Conf.*, 2007, pp. 1775–1780.
[15] T. Dierks and S. Jagannathan, "Output feedback control of a quadrotor UAV using neural networks," *IEEE Trans. Neural Netw.*, vol. 21, no. 1, pp. 50–66, Jan. 2010.
[16] M. Huang, B. Xian, C. Diao, K. Yang, and Y. Feng, "Adaptive tracking control of underactuated quadrotor unmanned aerial vehicles via backstepping," in *Proc. Amer. Control Conf.* , 2010, pp. 2076–2081.
[17] T. Lee, M. Leok, and N. H. McClamroch, "Nonlinear robust tracking control of a quadrotor UAV on SE (3)," *Asian J. Control*, vol. 15, no. 2, pp. 391–408, 2013.
[18] Y. Mitikiri and K. Mohseni, "An analytic solution to two quaternion attitude estimation problems," *IEEE Trans. Autom. Control,*, arXiv:1901.08905.
[19] Y. Mitikiri and K. Mohseni, "Modelling and control of a miniature, low-aspect-ratio, fixed-delta-wing, rudderless aircraft," in *Proc. AIAA Guid., Navigation, Control Conf.*, Kissimmee, FL, USA, Jan. 2018, Paper 2018-876.